Journal of Molecular Liquids 293 (2019) 111527

Contents lists available at ScienceDirect

Journal of Molecular Liquids

journal homepage: www.elsevier.com/locate/molliq

Does the partial molar volume of a solute reflect the free energy of hydrophobic solvation?

Anna Szymaniec-Rutkowska [a], Ewa Bugajska [a], Sławomir Kasperowicz [a,b], Kinga Mieczkowska [a], Agnieszka M. Maciejewska [a], Jarosław Poznański [a,*]

[a] Institute of Biochemistry and Biophysics, Polish Academy of Sciences, Pawińskiego 5a, 02-106 Warszawa, Poland
[b] Warsaw University of Technology, Faculty of Chemistry, Noakowskiego 3, 00-664 Warszawa, Poland

ARTICLE INFO

Article history:
Received 22 January 2019
Received in revised form 4 June 2019
Accepted 6 August 2019
Available online 07 August 2019

Keywords:
Partial molar volume
Hydrophobic effect
Halogenated benzotriazoles
Ligand binding
Thermal shift assay
Chromatographic Hydrophobicity Index

ABSTRACT

Halogenated heterocyclic ligands are widely used as the potent and frequently selective inhibitors of protein kinases. However, the exact contribution of the hydrophobic solvation of a free ligand is rarely accounted for the balance of interactions contributing to the free energy of ligand binding. Herein, we propose a new experimental method based on volumetric data to estimate the hydrophobicity of a ligand. We have tested this approach for a series of ten variously halogenated benzotriazoles, the binding affinity of which to the target protein kinase CK2 was assessed with the use of thermal shift assay. According to the hierarchical clustering procedure, the excess volume, defined as the difference between the experimentally determined partial molar volume and the calculated *in silico* molecular volume, was found to be distant from any commonly used hydrophobicity descriptors of the ligand. The excess volume, however, properly predicts solute binding affinity. On the way, we have proved that the binding of halogenated benzotriazoles to the protein kinase CK2 is driven mostly by hydrophobic interactions.

1. Introduction

Hydrophobic effect has been extensively studied for over 70 years [1–6]. It is so because of its extreme importance in a variety of physical and biological phenomena, including protein folding or binding of low-mass ligands. The first microscopic theory of hydrophobic interactions was formulated by Frank and Evans in 1945 [7]. They described the behavior of water molecules organized in an ice-like structure surrounding the apolar solute, which was further confirmed with the use of crystallography [8] and molecular dynamics [9]. In 1959, Kauzmann proposed that the physical properties of an aqueous hydrocarbon solution can be explained by the presence of the hydration shell, in which the water molecules are much more ordered than those in the bulk water [10]. Following this concept, Zamyatnin attributed the difference between the experimentally measured volume of the protein and the value estimated by the amino acid composition to the packing effect accompanied by the conformational changes of amino acid residues inside the protein with the possible contribution of solvation phenomena [11,12], and, since then, over than a hundred of various hydropathy scales for amino acid residues have been proposed to support the sequence-based prediction of specific protein properties (see: Ref. [13] for review).

A strong correlation between the free energy of hydration and the number of water molecules packed around a hydrophobic compound was shown by Hermann [14,15], however, at that time, there was no quantitative description of both molecular and macroscopic hydrophobic phenomena until Stillinger's applied Reiss' scaled particle theory (SPT) [16] to describe the thermodynamics of hydration [17]. The alternative general solvophobic theory has been proposed by Sinanoglu, who correlated the free energy of solvation with the surface tension of the solvent and the solute solvent-accessible area [18]. Finally, Lum, Chandler and Weeks analyzing the size-dependency of solute-water interaction, showed that the free energy of solvation for small solutes is proportional to the volume, while that for the larger ones remains proportional rather to the molecular surface [19].

The analysis of the radial distribution function (RDF) for water molecules identified in 105 highest-resolution protein structures showed that the solvation shell resembles rather liquid water than ice, however, the shape of the observed RDF maxima indicated that hydrating water is much more stable than the bulk one [20]. This was independently confirmed by molecular dynamics studies, in which properties of water solvating the solute molecule differ from those of the bulk solvent [21–24]. An increased water density determined *in silico* in the vicinity of the protein [25–27] was also confirmed experimentally with the use of X-ray solution scattering data [28,29], however, for neutron scattering, the same authors observed the opposite effect [28,29]. Infrared spectroscopic data demonstrated that small hydrophobic solutes make the

* Corresponding author.
E-mail address: jarek@ibb.waw.pl (J. Poznański).

https://doi.org/10.1016/j.molliq.2019.111527

proximal network of water-water H-bonds much more ordered than that in the bulky water [30,31], while an increased population of water molecules strongly bound to the solute is observed for proteins [32] or amino acids [33]. All in all, it indicates that hydrophobic effect, *i.e.* solute-induced changes in the organization of the solvation shell, including both static and dynamic properties, gather the thermodynamics of the molecule in an aqueous solvent.

Hydrophobic effect is of extreme importance in a drug design approach, especially for highly hydrophobic ligands, the binding affinity of which may be predominated by the unfavorable interactions of the free solute with an aqueous solvent. The effective inhibitory activity depends on the apparent free energy of protein-ligand interactions, the deconvolution of which to the contributions of direct protein-ligand interactions and the solvent-driven effect of desolvation (both for ligand and the protein) is difficult, and in most cases remains unresolved. Leo, Hansh and Elkins successfully used partition coefficients in octan-1-ol/water system (LogP) as a measure of solute hydrophobicity [34,35]. This approach has soon become fundamental, and since then LogP data routinely support drug design procedures. However, aqueous solubility (LogS) and pH-dependent distribution coefficient (LogD) are also commonly used. Partition coefficients usually correlates with ligand binding affinities [36,37], however, the dependency of ligand affinity on LogP is generally nonlinear, thus indicating an optimal drug hydrophobicity [2].

In the case of halogenated ligands, the exact contributions of halogen bonding, hydrophobic effect and halogen-induced changes in the solute electronic properties to the free energy of ligand binding cannot be extracted directly from the experimental thermodynamic data. It should be noted that, although the enthalpy of solute-solvent interaction can be determined calorimetrically by the combination of the enthalpy of solution and the enthalpy of sublimation, there is still no experimental method to estimate directly the entropic contribution to the solute-solvent interactions. It should also be stressed that, in order to improve the preliminary steps of drug design procedures, there is a strong need for at least a semi-quantitative method to assess these interactions. Here, we test our former model of hydrophobic solvation, in which the observed excess volume (β) that represents the difference between the experimentally measured partial molar volume and the estimated *in silico* molecular volume was attributed directly to the effect of the reorganization of water molecules in the solvation shell [38–42]. This extensive thermodynamic parameter was proposed as a measure of the free energy of the reorganization of water molecules surrounding the solute molecule. The application of the proposed model is now tested for five rationally selected bromo-benzotriazoles and their five chloro-analogues. The hydrophobicity of solutes was independently estimated from RP-HPLC retention times, the values of which were proven to correlate with LogP data [43]. We have also analyzed other physicochemical parameters that are routinely determined upon the early steps of drug design procedure (pK_a, $LogC_w$, LogP, LogS).

All tested ligands, which are the derivatives of the first-reported low-mass ATP-competitive inhibitor of protein kinase CK2, 4,5,6,7-tetrabromo-1*H*-benzotriazole [44], are expected to bind at the ATP-binding site of the catalytic domain of protein kinase CK2 (CK2α), so in this way we have assessed the applicability of various methods confronting the thermodynamic parameters determined for free ligands with their binding affinities deduced from the thermal shift assay.

2. Material and methods

2.1. General procedure for synthesis chloro-benzotriazoles

Commercially available chemicals were of reagent grade and used as received. 3-chlorobenzene-1,2-diamine (95%) was purchased from abcr (Karlsruhe, Germany), 4-chlorobenzene-1,2-diamine (97%) and 3,5-dichlorobenzene-1,2-diamine (97%) were purchased from Sigma Aldrich (Munich, Germany), 4,5-dichlorobenzene-1,2-diamine (95%) was purchased from Fluorochem (Hadfield, UK). All bromo-substituted benzotriazoles were synthesized according to the previously used methods [45,46]. 4,5,6,7-Tetrachloro-1*H*-benzotriazole was synthesized according to literature procedure [47].

Melting points (uncorrected) were determined in open capillary tubes, using a Büchi B504 apparatus. The reaction progress was monitored with the use of thin-layer chromatography (TLC) analysis using silica gel plates (Kieselgel, $60F_{254}$, E. Merck, Darmstadt, Germany). Column chromatography was performed on Silica Gel 60 M (0.040–0.063 mm, E. Merck, Darmstadt, Germany). High-resolution mass spectra were recorded on an LTQ Orbitrap Velos instrument (Thermo Scientific). NMR spectra were recorded in DMSO d_6; signal assignment for the chlorinated benzotriazoles based on the data already published for bromo-benzotriazoles [45,46,48]. The purity of all studied compounds was controlled with the use of HPLC twice: in isocratic conditions (2: 1 methanol: 20 mM ammonium formate, (AF) pH 6.5), and with the linear gradient of 20 mM AF pH 6.5 × 65–95% aq. MeOH over 30 min at a flow rate of 0.7 mL/min.

A solution of 10 mmol of the appropriate benzene-1,2-diamine in 3.5 mL of acetic acid (AcOH) and 1 mL of water was cooled to 0–5 °C, followed by the addition of 15 mmol of sodium nitrite in 2 mL of water. The mixture was stirred for 2 h at room temperature. After the completion of the reaction, a solvent was evaporated and the residue was co-evaporated with toluene (3 × 20 mL). The crude product was partitioned between water (20 mL) and ethyl acetate (20 mL), the organic phase was washed with the saturated solution of sodium hydrogen carbonate and dried over magnesium sulfate ($MgSO_4$). The products were purified by crystallization from nitromethane and/or by column chromatography on silica gel using a chloroform – methanol 97:3–95:5 v/v mixture as eluent. Reaction products were analyzed by use of mass-spectrometry (Waters Q-TOF Premier Mass Spectrometer) and NMR spectroscopy (Varian INOVA 500 Spectrometer, see Supp. Fig. 1). Purity of the products was assessed using internal standard quantitative NMR method (qNMR) [49]. It should be noted that the formal qNMR-derived purity determined for 4-BrBt, 4-ClBt, 5,6-Cl_2Bt and 5,6-Br_2Bt increased significantly upon addition a small amount of water to the DMSO solution, which increased proton exchange rates. This observation indicates that the nuclear relaxation process accompanying protomeric equilibrium (generally N1-H and N3-H forms predominates) significantly contribute to the obtained NMR spectra, the best proof of which is the strong broadening of the H-7 resonance line in 4-BrBt and 4-ClBt (Supp. Fig. 1A,B).

4-Chloro-1*H*-benzotriazole (4-ClBt): yield 550 mg (24%); mp. 170.6–172.1 °C (lit. 168.5–169.5 °C) [50]; HRMS (ESI): *m/z* $[M + H]^+$ calc. For $C_6H_5ClN_3$: 154.01665, 156.01370 found: 154.01665, 156.01362; ^{1}H NMR 500 MHz (DMSO d_6) δ [ppm]: 7.87 (bs, 1H, H-7); 7.50–7.57 (m, 2H, H-5,H-6: 7.56; assigned as ad, 1H, H-5, $J = 7.4$ Hz; 7.51 and at, 1H, H-6, $J = 7.4$ Hz); qNMR purity (P_{qNMR}): 89.3%; (Supp. Fig. 1B).

5-Chloro-1*H*-benzotriazole (5-ClBt): yield 400 mg (32%); mp. 158.7–159.8 °C (lit. 156–157 °C) [46,51]; HRMS (ESI): *m/z* $[M + H]^+$ calc. for $C_6H_5ClN_3$: 154.01665, 156.01370 found: 154.01665, 156.01363; ^{1}H NMR 500 MHz (DMSO d_6) δ [ppm]: 8.05 (s, 1H, H-4); 7.99 (d, 1H, H-7, $J = 8.8$ Hz); 7.50 (dd, 1H, H-6, $J_1 = 7.5$ Hz, $J_2 = 1.9$ Hz); P_{qNMR}: 93.9%; (Supp. Fig. 1D).

4,6-Dichloro-1*H*-benzotriazole (4,6-Cl_2Bt): yield 773 mg (49%); mp. 246–247.7 °C (lit. 245.5–246.5 °C) [52]; HRMS (ESI): *m/z* $[M + H]^+$ calc. for $C_6H_4Cl_2N_3$: 187.97768; 189.97473 found: 187.97748; 189.97446; ^{1}H NMR 500 MHz (DMSO d_6) δ [ppm]: 8.01 (s, 1H, H-7); 7.67 (d, 1H, H-5, $J = 1.4$ Hz); P_{qNMR}: 95.3%; (Supp. Fig. 1F).

5,6-Dichloro-1*H*-benzotriazole (5,6-Cl_2Bt): yield 690 mg (32%); mp. 263.5–266.5 °C (lit. 264–266 °C); HRMS (ESI): [48,53] *m/z* $[M + H]^+$ calc. for $C_6H_4Cl_2N_3$: 187.97768; 189.97473 found: 187.97752; 189.97451; ^{1}H NMR 500 MHz (DMSO d_6) δ [ppm]: 8.31 (s, 2H, H-4,H-7); P_{qNMR}: 84.0%; (Supp. Fig. 1H).

4,5,6,7-Tetrachloro-1*H*-benzotriazole (TCBt): yield 1.14 g (35%); mp. 258.4–261.5 °C (lit. 256–260 °C) [47,48] HRMS (ESI): m/z $[M + H]^+$ calc. for $C_6H_2Cl_4N_3$: 255.89973, 257.89678, 259.89383 found: 255.89938, 257.89645, 259.89348;

4-Bromo-1*H*-benzotriazole (4-BrBt): ^{1}H NMR 500 MHz (DMSO d_6) δ [ppm]: 7.91 (d, 1H, H-7, $J = 7.9$ Hz); 7.71 (d, 1H, H-5, $J = 7.4$ Hz); 7.45 (t, 1H, H-6, $J = 7.9$ Hz); P_{qNMR}: 96.7%; (Supp. Fig. 1A).

5-Bromo-1*H*-benzotriazole (5-BrBt): ^{1}H NMR 500 MHz (DMSO d_6) δ [ppm]: 8.20 (s, 1H, H-4); 7.93 (d, 1H, H-7, $J = 8.7$ Hz); 7.62 (dd, 1H, H-6, $J_1 = 8.8$ Hz, $J_2 = 1.8$ Hz); P_{qNMR}: 99.2%; (Supp. Fig. 1C).

4,6-Dibromo-1*H*-benzotriazole (4,6-Br_2Bt): ^{1}H NMR 500 MHz (DMSO d_6) δ [ppm]: 8.01 (d, 1H, H-7); 7.67 (d, 1H, H-5, $J = 1.5$ Hz); P_{qNMR}: 99.5%; (Supp. Fig. 1E).

5,6-Dibromo-1*H*-benzotriazole (5,6-Br_2Bt): 1H NMR 500 MHz (DMSO d_6) δ [ppm]: 8.45 (s, 2H, H-4,H-7); P_{qNMR}: 91.6%; (Supp. Fig. 1G).

3. Experimental

3.1. Solute properties in aqueous medium

3.1.1. pK_a determination

All ligands were titrated in the pH range of 3.5–10.5. Changes in absorption spectra recorded in the range 200–600 nm (Perkin Elmer Lambda 25 UV–vis spectrometer) were further analyzed globally according to the Henderson-Hasselbach formula, as proposed previously [45]; albeit the appropriate numerical model was implemented in Origin (www.originlab.com).

3.1.2. Aqueous solubility

The solubility of each benzotriazole derivative was determined at pH 8 in 25 mM Tris-HCl buffered solution. The suspensions, shaken at 25 °C for 72 h using Eppendorf Thermomixer Comfort, were then centrifuged and the solute concentration in the supernatant was determined from the UV–vis spectra of diluted solution (200–600 nm).

3.1.3. Chromatographic hydrophobicity index

Reverse phase HPLC analysis (RP-HPLC) was performed using a Knauer dual pump system equipped with a multi-channel UV spectrophotometer based on a diode array technology detector managed by ClarityChrom controller version 6.1.0.130. Separations were performed on a Waters Nova-Pak® C18, 60 Å, 4 μm, 4.6 × 250 mm, cartridge column, at a flow rate of 0.6 mL × min^{-1}, at 25 °C (working pressure ~12 MPa), with detection at 280 nm. An isocratic mobile phase composed of methanol and 20 mM aqueous ammonium formate (pH 6.5 or 8.0) in proportion either 2:1 or 7:3 (v:v) was applied. RP-HPLC-derived retention times, T_{ret}, were then converted to log(τ) scale according to the relation $\tau = (T_{ret} - T_0) / T_0$, in which the retention time of the unretained solvent, T_0, was estimated to 300 s.

3.2. QM methods

Ab initio calculations were done for the monoanionic form of all halogenated benzotriazoles, and for the two asymmetric protonation states of their neutral form using Firefly version 8.2 (Alex A. Granovsky, Firefly version 8, http://classic.chem.msu.su/gran/firefly/ index.html), the code of which was partially based on GAMSESS US [54]. The initial coordinates of nine chloro-derivatives, adopted from those of their bromo-analogues by the adjustment of C-Cl distance to 1.73 Å, were optimized using the DFT B3LYP functional with 6-31G(d,p) basis set. The contribution of solute-solvent interaction was estimated using the polarizable continuum model (PCM) [55]. The dissociation of the triazole proton, $\Delta G_{diss} = G_{neutral} - G_{monoanio} - G_{hydr}(H^+)$, and the solvation of the anionic form, ΔG_{int}, were analyzed in the terms of difference in the free energy with $G_{hydr}(H^+)$ taken as −262.3 kcal/mol [56]. Molecular volume (V_{mol}) and the volume of the solvation shell (V_{solv}) were calculated using the algorithm of tessellation originally implemented in the GEPOL [57].

3.3. Physicochemical ADME parameters

The larger set of parameters was determined with SwissAdme server [58]. The matrix of squared pairwise Pearson's correlation coefficients calculated for each pair of parameters was subjected to hierarchical cluster analysis according to Ward's minimum variance method [59] implemented in R package [60] (www.R-project.org).

3.4. Thermal shift assay

All measurements were carried out with Varian Cary Eclipse spectrofluorometer equipped with a variable-temperature four-cell holder dedicated for 10 mm path length cuvettes. Protein emission was monitored at 335 nm (excitation at 280 nm) in temperature range of 20 to 80 °C with 1 °C/min heating rate. The catalytic subunit of human protein kinase CK2 (hCK2α), was expressed and purified according to the method described previously [61]. The protein sample was diluted with 25 mM Tris-HCl (pH 8, 0.5 M NaCl) to the required concentration of 0.25 μM. All ligands, initially dissolved in DMSO, were added to the protein solution in 10 fold excess (2.5 μM), and the resulting solutions were further supplemented with DMSO to keep its final concentration constant (2%). The temperature-induced changes of protein fluorescence, F(T), were analyzed according to the model of two-state transition [62], implemented in Origin (www.origin.com) in the form:

$$\begin{aligned} F(T) &= p_{unf} * F_{unf}(T) + \left(1 - p_{unf}\right) * F_{fold}(T) p_{unf} \\ &= \{1 + \exp(\Delta G/RT)\}^{-1} \Delta G = \Delta H_{unf} + \Delta C_p * (T - T_m) + T \\ &\quad * \Delta S_{unf} + \Delta C_p * \ln(T/T_m) \Delta H_{unf} \\ &\quad + T_m * \Delta S_{unf} \\ &= 0 \end{aligned} \quad (1)$$

where F_{unf} and F_{fold} are the low- and high-temperature linear asymptotes of F(T), respectively. For each experiment these asymptotes were individually fitted, while the other thermodynamic parameters: melting temperature (T_m), the enthalpy of unfolding (ΔH_{unf}) and heat capacity change upon denaturation (ΔC_p) were optimized globally for all data collected for a given ligand (Supp. Fig. 2).

3.5. Density measurements

Partial Molar Volumes were estimated on the basis of the experimentally determined concentration-density dependency of the aqueous solutions of compounds in 50 mM phosphate buffer at pH 11. Such a high pH value was set, because the limited solubility of some halogenated bezotriazoles at pH 8 (*e.g.* TBBt or 5,6-Br_2Bt) precluded precise measurements. For each compound the exact densities for a series of the dilutions of the stock solution were measured on high-precision density meter Anton Paar DMA 5000 M, in which the U-shaped tube filled with a sample solution is electronically excited to oscillate. According to supplier recommendation, the system was daily checked for empty tube (*i.e.* scaled on the air density), and for the reference liquid density standard sample of Anton Paar's certified ultra-pure water. All samples were degassed before measurement.

1. Theory

According to the iceberg hypothesis of Frank and Evans, hydrophobic solutes are expected to order surrounding water molecules [7]. Thus, the difference between the experimentally determined partial molar volume and the estimated *in-silico* molecular volume reflects the net effect of the solute-induced reorganization of the solvation shell [38–42]. Our previous studies clearly demonstrated that for extremely non-polar solutes the apparent density of the solvation shell

Table 1
Thermodynamic parameters calculated (ΔG_{ioniz}, ΔG_{int}, V_{mol}) and determined experimentally (V_2^0, β, pK_a, log(C_w) and log(τ)) for halogenated benzotriazoles in aqueous solution, and temperature of thermal denaturation of their complexes with hCK2α (T_m).

Subst. pattern	ΔG_{ioniz}	ΔG_{int}	V_{mol}	V_2^0	β	pK_a	log(C_w)	log(τ)	T_m
	[kcal/mol]		[cm^3/mol]				[M]	pH = 8	[°C]
apo	–	–	–	–	–	–	–		47.9 ± 0.1
CHHH	35.4	−55.3	71.4	127.4 ± 0.4	56.0 ± 0.4	7.17	−1.98	−0.71	47.6 ± 0.2
HCHH	37.4	−52.7	71.4	132.3 ± 0.6	60.9 ± 0.6	7.73	−2.17	−0.49	48.5 ± 0.1
CHCH	33.3	−47.9	80.7	143.7 ± 0.5	63.0 ± 0.5	6.19	−2.57	−0.49	49.6 ± 0.1
HCCH	35.3	−47.4	80.6	134.4 ± 0.6	53.8 ± 0.6	6.83	−3.33	−0.37	51.4 ± 0.1
CCCC	29.1	−40.7	99.1	166.7 ± 0.5	67.6 ± 0.5	5.16	−4.64	−0.07	50.2 ± 0.1
BHHH	36.1	−54.8	74.9	139.0 ± 0.3	64.1 ± 0.3	7.08	−2.41	−0.65	48.9 ± 0.2
HBHH	38.2	−51.7	75.1	133.7 ± 0.6	58.6 ± 0.6	7.55	−2.56	−0.40	48.7 ± 0.1
BHBH	34.1	−47.1	87.9	151.7 ± 0.6	63.8 ± 0.6	6.38	−3.63	−0.37	50.1 ± 0.1
HBBH	36.4	−46.4	87.7	147.3 ± 0.5	59.6 ± 0.5	6.93	−3.64	−0.29	53.1 ± 0.1
BBBB	30.9	−40.8	113.2	192.0 ± 1.5	78.8 ± 1.5	5.10	−3.66	−0.00	54.1 ± 0.1

approaches that of ice [38,39,41], and suggested that the excess volume (β) may be regarded as a measure of solute hydrophobicity [40,42]. Here we tested the latter hypothesis on biochemically relevant ligands using more sensitive apparatus and applying the improved method of the analysis of volumetric data.

2. Calculations

The standard analysis of density data based on the apparent molar volume [63], V_φ, (Eq. 2) was found inapplicable due to the limited aqueous solubility of all studied highly hydrophobic compounds and the hardly reproducible composition of buffered solution constituing a 'pure solvent'.

$$V_\phi = \frac{10^3}{m\rho\rho_0}(\rho_0 - \rho) + \frac{M}{\rho} \tag{2}$$

where m is the molal concentration of the solute (mol/kg), M is the molar mass, and ρ and ρ_0 are the density of the solution and the 'pure solvent', respectively. However, partial molar volume, V_2^0, can be estimated directly from the density data:

$$V_2^0 = V_\phi^{m\to 0} = \frac{M}{\rho_0} - \frac{10^3}{\rho_0^2} * \frac{\partial\rho}{\partial m}\Big|_{m=0} \tag{3}$$

where ρ_o and $\partial\rho/\partial m$ are the intercept and slope in the linear approximation of ρ(m). This approach includes additional auto-correction for the density of the 'pure solvent', which cannot be sufficiently reproduced in independent buffer preparations. The numerical model based on Eq. (3) was implemented in Origin (www.origin.com).

We have extensively tested the reproducibility of measurements and sensitivity to independent buffer preparations (Supp. Fig. 3A, and Supp. Table 1) and found that the global analysis at 3 close temperatures improves precision when linear relation $V_2^0(T)$ is assumed (see Supp. Fig. 3B and Supp. Table 1).

The model was also fitted independently to each dataset, and the resulting set of partial molar volume values did not differ significantly from the value obtained by global fitting to all experiments. This latter approach resulted, however, in the reduced uncertainty (standard deviation) of the estimated V_2^0.

4. Results and discussion

We introduced new extensive thermodynamic parameter, β, which can be interpreted as a measure of solvation free energy and thus can be used to determine effective compounds' hydrophobicity. We have tested our model with the rationally chosen halogenated derivatives of benzotriazole, which are expected to be the competitive inhibitors of the human protein kinase CK2. The particular patterns of halogen substitution (see Scheme 1) were selected to affect significantly

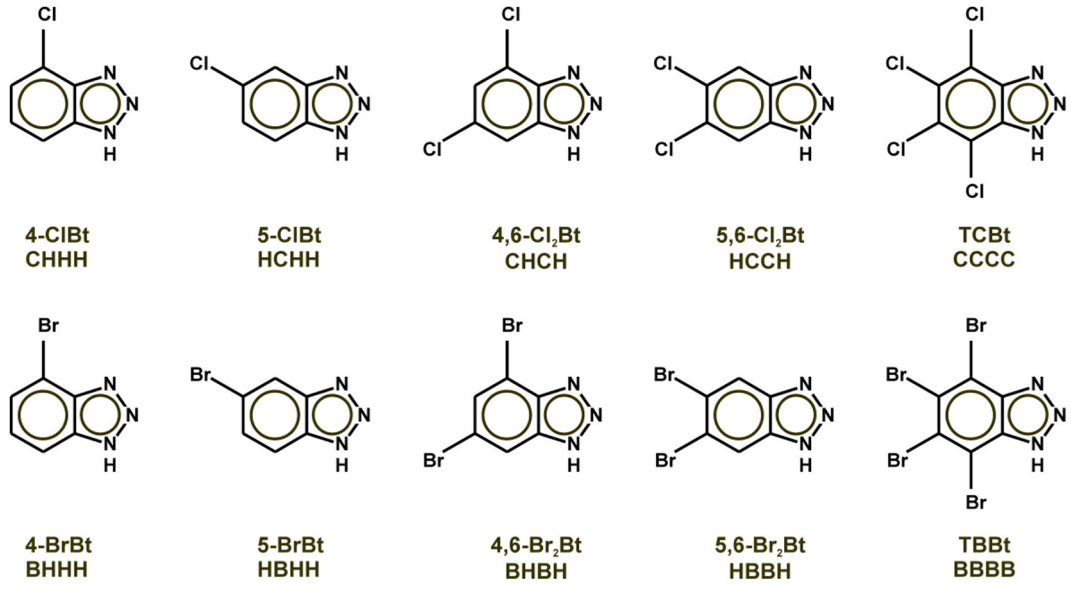

Scheme 1. Chemical structures of the compounds used in the study.

physicochemical properties and biological activity, however, it should be stressed that the halogenation of any solute molecule generally increases its hydrophobicity. To overcome this problem, in parallel we studied chlorinated derivatives that stood the reference set for the series of brominated benzotriazoles. For the latter ones, we have already determined physicochemical [45], biochemical [64] and thermodynamic [61,65,66] parameters describing their interaction with the catalytic subunit of human protein kinase CK2 (hCK2α). Chlorinated benzotriazoles should display similar physicochemical properties, however they are less hydrophobic than their brominated counterparts and hence their solubility in the aqueous solution should be increased. They are also expected to display lower propensities for the formation of halogen bonds in protein–ligand systems [67–70].

4.1. QM calculations

QM-calculations proved that electronic properties for both series of halogenated benzotriazoles are similar in aqueous medium (Table 1) including the free energy for the dissociation of the triazole proton (Fig. 1A), and the free energy of solute-solvent interactions for both neutral (not shown) and monoanionic (Fig. 1B) forms, both of which are highly correlated for the pairs of the corresponding isomeric forms of chloro- and bromo-benzotriazoles.

Following the above correlations, two mono-substituted (4-ClBt, 5-ClBt), two bi-substituted (4,6-Cl_2Bt, 5,6-Cl_2Bt) and per-chlorinated TCBt, together with their five bromo-analogues (Scheme 1), were selected for further biophysical and biochemical studies.

Three of these chlorinated benzotriazoles are the analogues of the efficient bromo-benzotriazole ligands of hCK2α (5-BrBt, 5,6-Br_2Bt and TBBt) [66], while the two remaining counterparts (4-BrBt and 4,6-Br_2Bt) were found substantially less active [61].

4.2. Physicochemical properties in solution

Eleven *in silico* determined ADME parameters (MW - molecular weight; MR - molar refraction index, iLOGP, XLOGP3, WLOGP, MLOGP, Silicos-IT LogP; Consensus LogP; ESOL LogS; Ali LogS; and Silicos-IT LogSw) together with molecular volume (Vmol) were analyzed for the set of nine chloro- and nine bromo- benzotriazole derivatives. Most of these parameters, summarized in Supp. Table 2, were found extremely correlated (Supp. Fig. 4). Ten of them cluster into two groups consisting of ESOL LogS, MR, V_{mol} and Silicos-IT LogSw, and Silicos-IT, LogP, Ali LogS, XlogP3, MLOGP, WLOGP and Consensus LogP, respectively, while iLOGP and MW are less correlated with the other ones. It should be also noted that iLOGP [71] is the only parameter that differentiates between isomers (Fig. 1C), which, however, substantially differ both in their physicochemical properties in the aqueous solution [45] and in affinity towards hCK2α [61] (Table 1).

The pK_a values for the dissociation of the triazole proton has already been determined for all the possible bromination patterns of the benzene ring of benzotriazoles [45]. Importantly, the values determined for the five selected chlorine derivatives (Table 1) are highly correlated with those for the corresponding bromo-analogues (Fig. 1D). This clearly confirms that the electronic effect associated with the replacement of all the bromine atoms of the bromo-benzotriazole with chlorine remains uniform for the whole set of analyzed compounds. In addition, experimental Log(C_w) is reasonably correlated with estimated *in silico* LogS ($R^2 = 0.77$ for Silicos-IT Log Sw; 0.95 when TBBt was excluded, Fig. 1F). So, a major disagreement involving the experimental solubility of TBBt must result from intensive (nano)aggregation, the existence of which, confirmed with the use of DLS technique [66], enhances apparent solubility.

The correspondence of *in silico* and experimentally derived parameters confirms that all tested benzotriazole derivatives may be regarded representative for testing application of thermodynamic parameters, to characterize the physicochemical properties of other compounds.

4.3. Density measurements – partial molar volumes of the monoanionic form of variously halogenated benzotriazoles

Experimental data was collected for benzotriazole, its five chloro- and five equivalent bromo-derivatives at 20, 25 and 30 °C (Supp. Table 3). All the measurements were carried out in the aqueous solution buffered at pH 11, so volumetric data concern the monoanionic form of the solute. Such a high pH was applied to enhance solubility and to prevent possible aggregation, the existence of which at the moderate pH of 8 has been already proven for TBBt [66]. According to F-test [72], the concentration-density relation was found linear for all compounds, so Eq. (3) was used to estimate V_2^0. The intercept, which corresponds to the density of the 'pure solvent' (buffer) slightly differs between particular samples, thus clearly exemplifying the advantages of the proposed method of data analysis (see Supp. Table 1 and Supp. Fig. 3 for details). As expected, partial molar volume generally varies with temperature, albeit the first-order linear approximation was always found sufficient by F-test. Finally, V_2^0 and $\partial V_2^0/\partial T$ were optimized globally for each compound, while 'poor solvent' density was fitted individually for each dataset.

For each compound the expected molar volume (V_{mol}) and the volume of the solvation shell (V_{solv}) were estimated *in silico* on the basis of its modeled structure and atomic radii (see QM calculations). We interpret the difference between measured partial molar volume (V_2^0) and the expected molecular volume (V_{mol}) as the result of specific solute-solvent interactions. This difference mostly reflects solute-induced variation in the average organization of water molecules that solvate a hydrophobic species [38,39]. This excess volume, $\beta = V_2^0 - V_{mol}$, is the extensive parameter, which can thus be interpreted as a measure of solvation free energy, while $\alpha = -\beta/V_{solv}$ describes the apparent solute-induced change in the solvent density within the solvation shell constituting apparent measure of solute polarity [40,41].

As expected, partial molar volume (V_2^0) increases with the number of halogen atoms attached to the benzene ring of benzotriazole, and is strongly correlated with calculated *in silico* molecular volume, V_{mol} ($R^2 = 0.98$, Fig. 2A).

However, the excess volume, β, is substantially less correlated ($R^2 = 0.83$, Fig. 2B), which makes it possible to support the standard QSAR approach. It should also be mentioned that β is always larger for bromo-benzotriazoles than for their chloro-analogues, thus, clearly confirming that bromine is much more hydrophobic than chlorine.

4.4. Chromatographic hydrophobicity index

HPLC technique becomes fast and efficient alternative to the standard LogD determination in octan-1-ol/water system [73–75]. In order to assess the applicability of the method to so hydrophobic ligands we have tested mobile phase using two methanol:buffer ratios (2:1 and 7:3 v/v). RP-HPLC runs were performed at pH 8 to estimate solute properties in the same conditions, at which other measurements were done. The same experiments were repeated at pH 6.5 to monitor the possible contribution of solute ionic state to the apparent hydrophobicity. To asses reproducibility, two additional runs were done at pH 6.5 (2:1 v:v) using the other column of the same type. Retention times determined at a given pH are strongly correlated ($R^2 > 0.98$), while those obtained at different pH are clearly less, but still significantly correlated ($R^2 =$ 0.80–0.86, see Fig. 4 below). All HPLC-derived data are summarized in Supp. Table 4.

4.5. Thermal shift assay

We have also tested the applicability of the excess volume (β) in the analysis of the hydrophobic contribution to the stability of protein-ligand complexes. The latter was assessed as a temperature shift in the fluorescence recorded upon the thermal unfolding of the appropriate complex (Thermal Shift Assay). In the case of small rigid ligands any

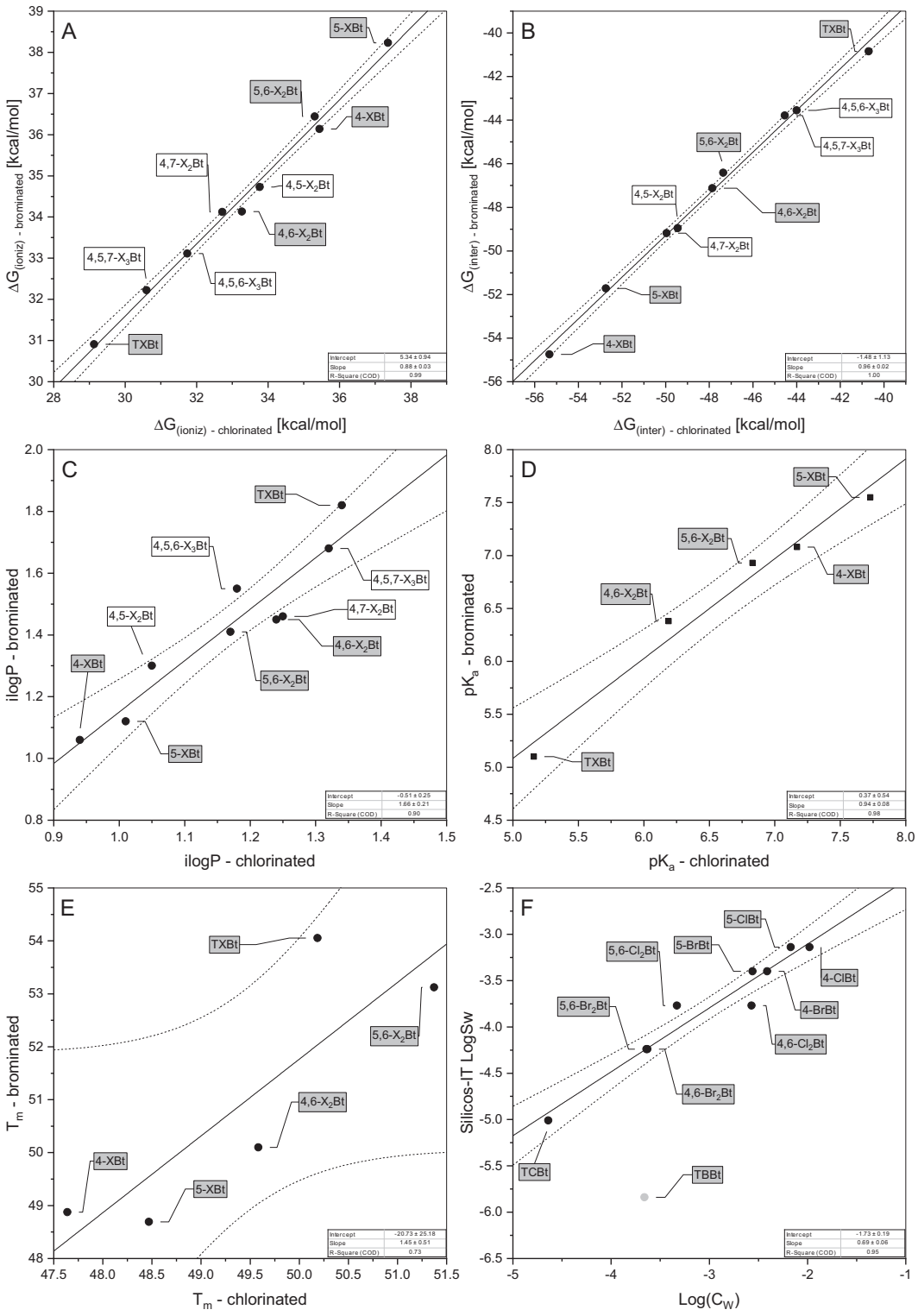

Fig. 1. Correspondence of the free energy for the dissociation of the triazole proton of selected brominated benzotriazoles with their chlorinated counter-partners (A), energy of solute-solvent interaction determined for anionic state of halogenated benzotriazole (B), in silico partition coefficient - iLOGP (C), experimentally determined pK_a values (D), melting temperatures – T_m (E) and correlation of experimentally determined solubility – $Log(C_W)$ and in silico Silicos-IT $LogS_W$ (F). Free energy values were determined ab initio for all nine possible bomination/chlorination patterns of the benzotriazole benzene ring. The pairs of isomers selected for the further experimental studies are denoted in gray.

increase in the temperature of protein unfolding upon ligand addition is indicative of the binding – the stronger ligand binding to the protein the higher is the middle-point temperature of the transition (T_m). For the *apo* form of hCK2α, and for its complexes with halogenated benzotriazoles, all the experimental thermal denaturation curves agree with the simplest model of two-state transition (Supp. Fig. 2). In the case of six ligands (4,6-Cl_2Bt, 5,6-Cl_2Bt, TCBt, 4,6-Br_2Bt, 5,6-Br_2Bt, TBBt), the thermal stability of their complexes significantly exceeds that of the *apo* form of hCK2α ($\alpha < 10^{-6}$), while the four remaining ones do not affect protein unfolding, thus indicating that they virtually do not bind to hCK2α at the tested concentration (Table 1). Contrary to QM-derived and physicochemical parameters, no significant T_m

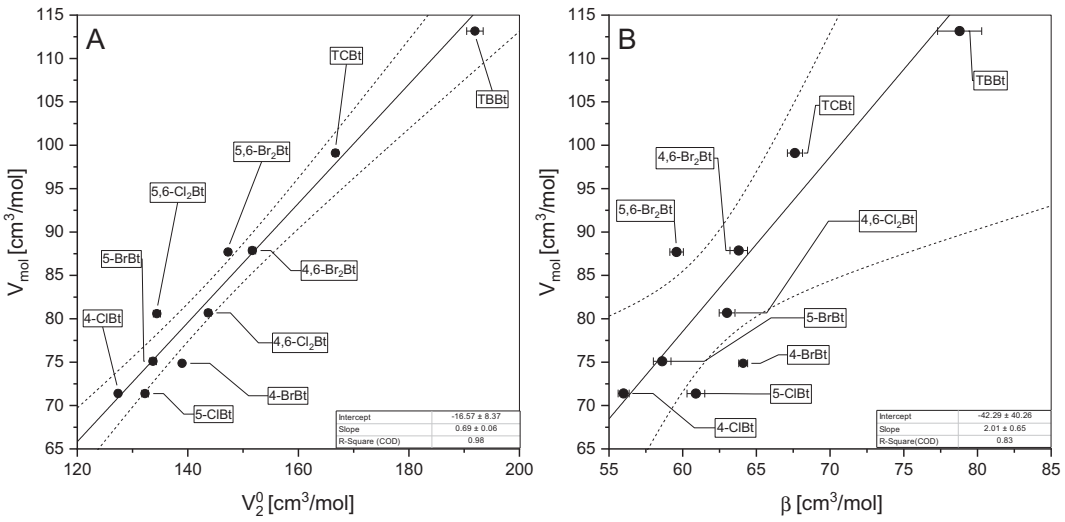

Fig. 2. Correlation of estimated in silico molecular volume, V_{mol}, with experimentally determined partial molar volume, V_2^0 (A) and the resulting excess volume, β (B).

correspondence between chloro- and bromo-benzotriazoles is observed (Fig. 1E). This clearly indicates that the replacement of bromine with chlorine individually affects different complexes. Since a balance of electrostatic and hydrophobic interactions was found to contribute predominately to the binding of bromo-benzotriazoles to hCK2α [61,65], only moderate trend for Br replacement with Cl could be observed.

According to our understanding of accessible thermodynamic data [61,66], we expected a general monotonic relation between β for the free solute and denaturation temperature of the protein-ligand complex (T_m). So, the greater hydrophobicity of the ligand, the stronger binding to the protein and the higher temperature at which the complex unfolds. In fact, the relation $T_m(\beta)$ was found almost linear (Fig. 3A). The uniform trend observed for eight ligands is indicative of a common pattern of interactions driving the formation of the protein-ligand complex, predominated by the hydrophobicity of the free solute. Consequently, the complexes of the two remaining ligands (5,6-Br_2Bt, and 5,6-Cl_2Bt), the data of which substantially deviates from the correlation line, are indicative of an alternative pattern of interactions within the complex that additionally stabilize ligand-bound state. At the moment, it could be hypothesized that the complexes of these two ligands are stabilized by intermolecular halogen bond(s) formed with the hinge region of hCK2α, as it was observed for the numerous halogenated ligands bound by a protein kinase [68,69,76–78].

Interestingly, the predictive power of the excess volume was found close to that of iLOGP, and significantly stronger than that of any other parameter (Fig. 3). We have also analyzed correlation matrix determined for 25 parameters describing both *in silico* and the experimentally derived properties of ten analyzed halogenated benzotriazoles (Fig. 4).

All *in-silico* determined LogS/LogP values are clustered together, however they are also correlated with molecular volume (V_{mol}), which, according to LCW theory, is a measure of hydrophobic solvation [19], and an experimentally determined partial molar volume (V_2^0), which should be considered as the experimental equivalent of V_{mol}. Experimental pK_a for the dissociation of the triazole proton is clustered with QM-derived free energy for the dissociation of that proton, but also with the QM-derived free energy of solvation. Interestingly, all these three parameters cluster with the excess volume, β, thus clearly pointing that hydrophobic interactions are predominately affected by the ionic state of the solute molecule.

As expected, HPLC-derived hydrophobicity data are clustered together, however, all these parameters are also substantially correlated with the experimental $LogC_w$ and QM-derived free energy of solute-solvent interaction, ΔG_{int}.

The last two parameters: molecular weight (MW) and iLOGP are clustered together with the denaturation temperature of protein-ligand complexes (T_m), which is a measure of ligand affinity. T_m also remains relatively close to $LogC_w$ and HPLC-derived hydrophobicity. Altogether, it clearly confirms that the binding of halogenated benzotriazoles is mostly driven by hydrophobic interactions.

In this view, the complexes of 5,6-Br_2Bt, and 5,6-Cl_2Bt, both of which disagree with a general trend observed for T_m as a function of β (Fig. 3A), experimental $LogC_w$ (Fig. 3B), chromatographic hydrophobicity index (Fig. 3C), and QM-derived ΔG_{int} (Fig. 3D), must be stabilized by another type of interactions. In fact, we identified two alternative locations of 5,6-Br_2Bt in the recently solved structure of its complex with *Z. mays* CK2α (5TS8, Fig. 5A), while no such effect is observed for TBBt bound to the same protein (1 J91, Fig. 5B) [79].

The two poses of 5,6-Br_2Bt reflect competition between halogen bonds formed with carbonyl oxygen atoms of Glu114 and Val116 located in the hinge region (red arrows in Fig. 5A) and electrostatic interactions with the salt bridge formed by Lys68 and Glu81 (magenta arrow in Fig. 5A), while TBBt interacts only with Lys68/Glu81 (magenta arrow in Fig. 5B). Alternative ligand poses identified in the case of 5,6-Br_2Bt are commonly observed in already resolved complexes of a protein kinase with a halogenated ligand [69]. In this context, the increased stability observed for hCK2α complex with 5,6-Br_2Bt may be regarded indicative of the halogen bonding. It must be, however, noted that the sequence of *Z. mays* CK2α differs from that of hCK2α, so the thermodynamic observations cannot be directly related to the structural data. Nonetheless, the coexistence of two alternative poses for 5,6-Br_2Bt indicates that, at least for *Z. mays* CK2α, the thermodynamic contribution of two halogen bonds is comparable to that of electrostatic interactions, which however, predominate for TBBt.

5. Conclusions

The proposed new thermodynamic parameter β (excess volume) correlates with the temperature of denaturation of the protein-ligand complex (T_m), which is the commonly accepted indicator of the strength of protein-ligand interaction. However, T_m is relatively independent of the standard set of *in silico* derived physicochemical parameters that are routinely used in drug design approach. For such hydrophobic ligands, an uncontrolled spontaneous solute (nano)aggregation [66] precludes the application of apparent ligand solubility as a measure of hydrophobicity. The same may to some extent concern experimental partition coefficients (LogP and LogD). So, we conclude that the excess volume may constitute an alternative to

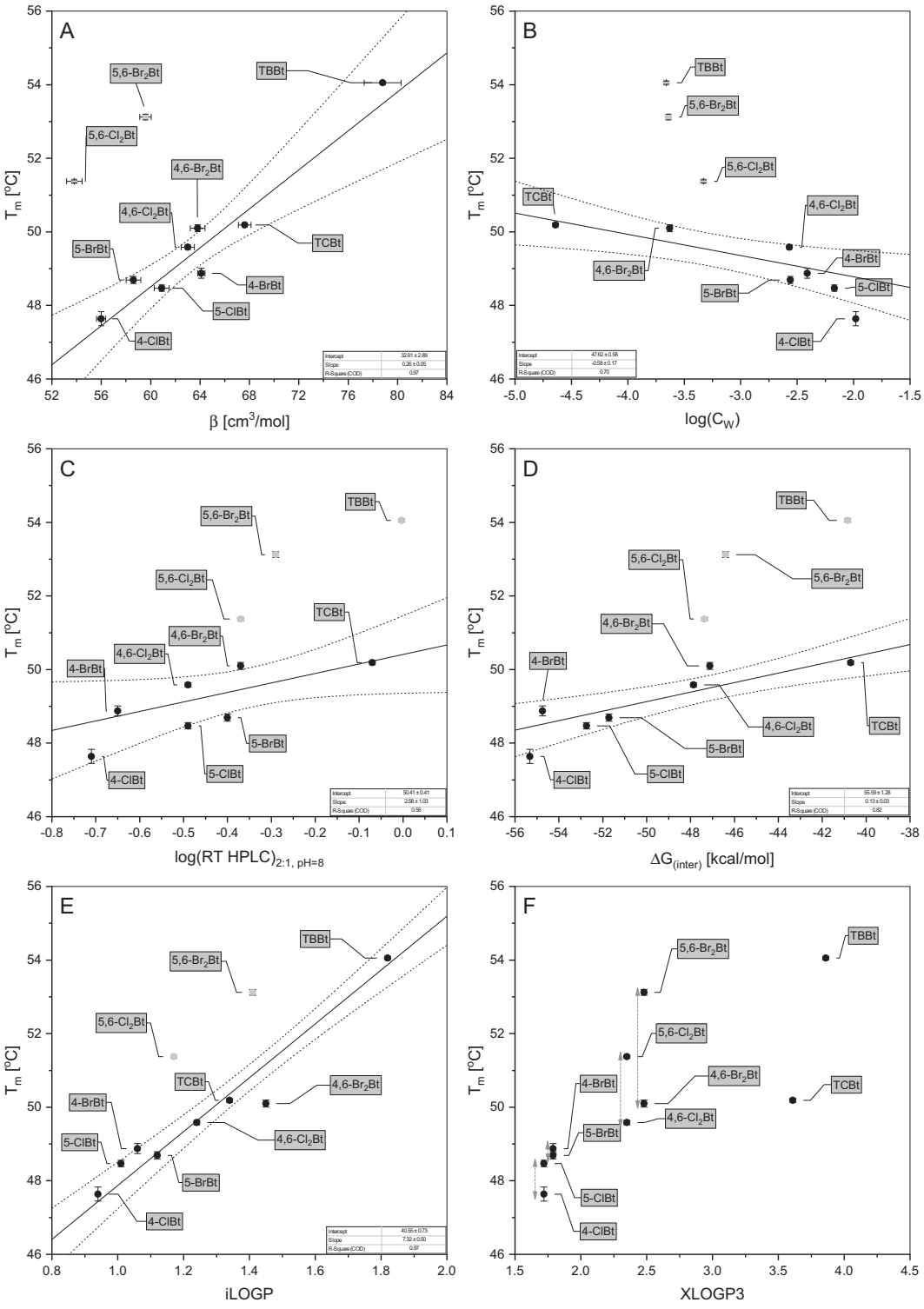

Fig. 3. Correspondence of temperature of unfolding, T_m, for the hCK2α complexes with the excess volume, β (A) and representative physicochemical parameters: log(C_w) (B), iLOGP (E) and XLOGP3 (F, compounds with the same halogenations pattern involving different halogens are denoted by gray arrows) and HPLC-derived hydrophobicity (C, log(τ) assessed for 2:1 methanol:aqueous buffer mobile phase at pH 8), and QM-derived free energy of solute-solvent interacton (D, $\Delta G_{(inter)}$). Complexes of hCK2α with 5,6-Cl_2Bt and 5,6-Br_2Bt, both of which display unpredictably high T_m, are putatively stabilized by other specific pattern of intermolecular interactions.

quantifying the hydrophobicity of the solute, and also to estimating the contribution of hydrophobic effect to overall free energy for ligand binding. Finally, the large positive excess volumes determined for all studied compounds indicate that the structure of water in the solvation shell is disrupted and, in agreement with the iceberg concept of Frank and Evans, its average density is significantly lower than that of the bulky solvent. The determined values of excess volume can therefore be directly used to test the quality of various models of aqueous solvents.

Author contributions

A.S-R. designed, performed and analyzed all density measurements, characterized the physicochemical properties of solutes and wrote the

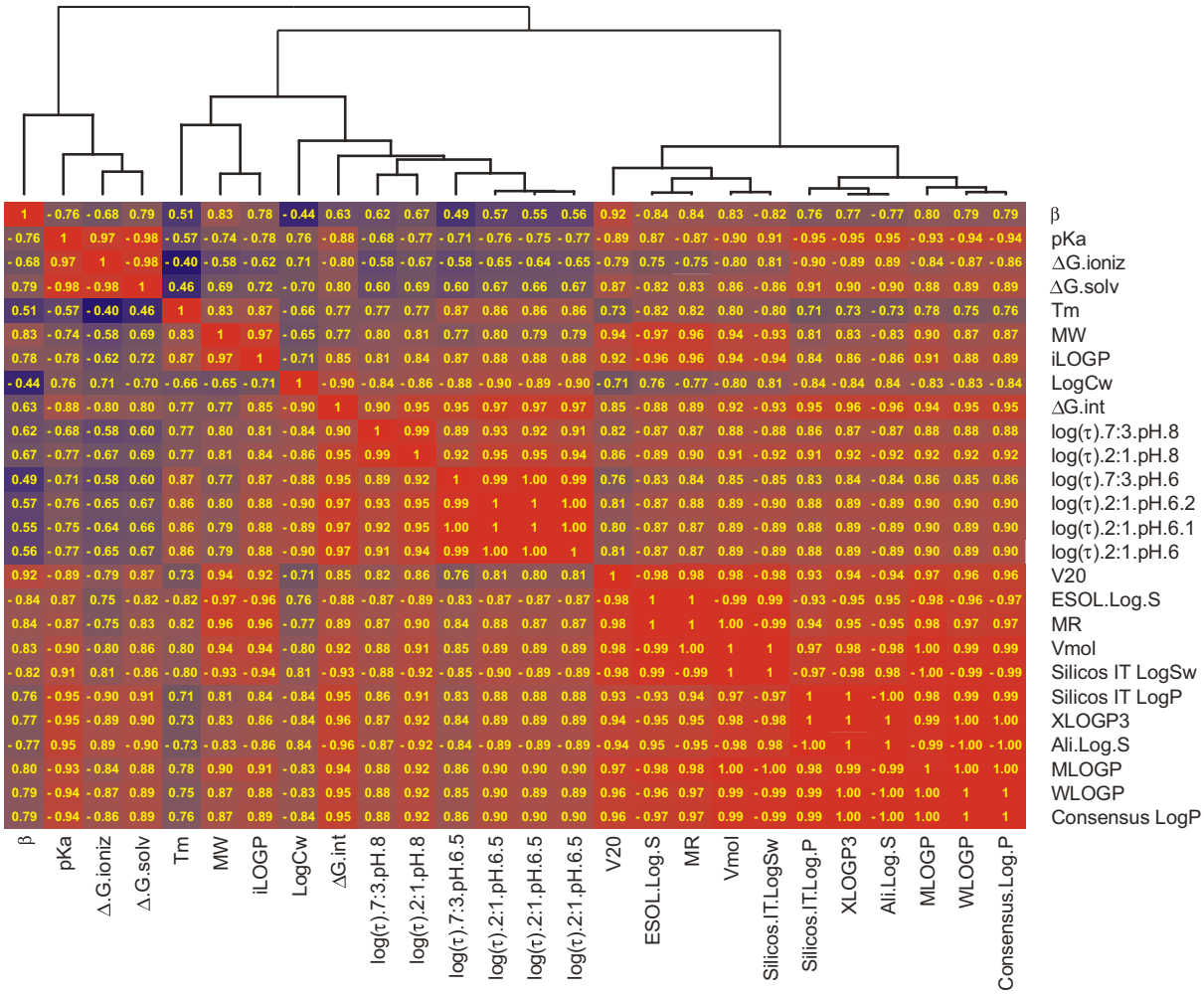

Fig. 4. Correlation matrix for the physicochemical parameters determined both in silico and experimentally (denaturation temperature of hCK2α complex with a given ligand, T_m, partial molar volume, V_2^0, exces volume, β, aqueous solubility at pH 8, LogCw, HPLC-derived hydrophobicity, log(τ), and pK for dissociation of the triazole proton. Hierarchical clustering was done for the matrix of variance using Ward's minimum variance method.

manuscript; E.B. expressed and purified protein samples, performed and analyzed Thermal Shift Assay experiments; S.K. and K.M. synthesized, purified and characterized benzotriazole derivatives; A.M.M. assessed the purity of samples, designed and performed HPLC experiments. J.P. performed QM calculations, analyzed the structures of CK2 complexes accessible in PDB, analyzed all experimental data and wrote the manuscript. All the authors read and approved the final manuscript.

Abbreviations

hCK2α
catalytic subunit of human protein kinase CK2
QM quantum mechanics
4-ClBt 4-chloro-1*H*-benzotriazole
5-ClBt 5-chloro-1*H*-benzotriazole
4,6-Cl_2Bt 4,6-dichloro-1*H*-benzotriazole
5,6-Cl_2Bt 5,6-dichloro-1*H*-benzotriazole
TCBt 4,5,6,7-tetrachloro-1*H*-benzotriazole
4-BrBt 4-bromo-1*H*-benzotriazole
5-BrBt 5-bromo-1*H*-benzotriazole
4,6-Br_2-Bt 4,6-dibromo-1*H*-benzotriazole
5,6-Br_2Bt 5,6-dibromo-1*H*-benzotriazole
TBBt 4,5,6,7-tetrabromo-1*H*-benzotriazole
MR molar refraction index
DLS dynamic light scattering
RP-HPLC reverse-phase high-performance liquid chromatography
LCW Lum-Chandler-Week theory of hydrophobic solvation
PCM polarizable continuum model
ADME absorption, distribution, metabolism, and excretion - parameters used in pharmacokinetics and pharmacology

Acknowledgments

This work was supported by the Polish National Science Centre grants 2015/19/B/ST4/02156 and 2017/25/B/ST4/01613. The used equipment was sponsored in part by the Centre for Preclinical Research and Technology (CePT), a project co-sponsored by the European Regional Development Fund and Innovative Economy, The National Cohesion Strategy of Poland. Synchrotron data collections were partly funded by the Seventh Framework Programme of the European Community (FP7/2007-2013) under the BioStruct-X grant agreement (N°283570). Dr. Maria Winiewska-Szajewska, Dr. Anna Piasecka-Fricke and Dr. Honorata Czapinska are acknowledged for the determination of crystal structure of 5,6-Br_2Br complex with *Z. mays* protein kinase CK2. Special thanks to Prof. Matthias Bochtler for stimulating discussions.

Appendix A. Supplementary data

Supplementary data to this article can be found online at https://doi.org/10.1016/j.molliq.2019.111527.

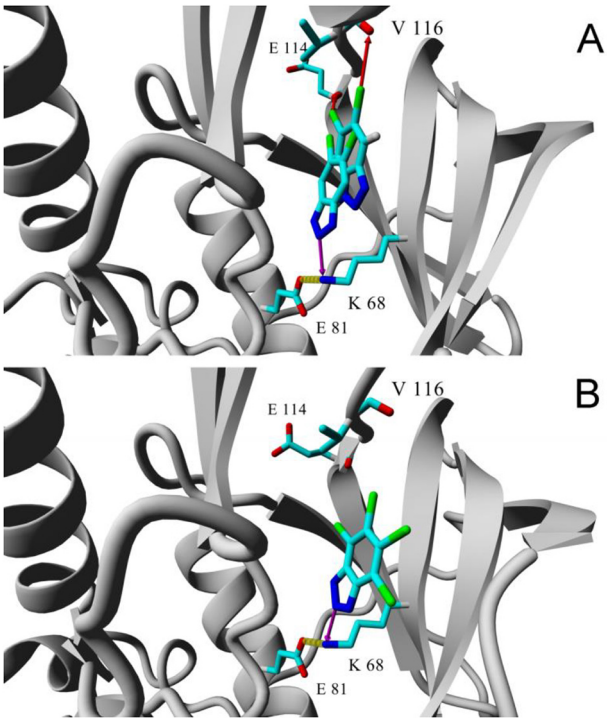

Fig. 5. Binding modes observed for complexes of the catalytic subunit of Z. mays protein kinase CK2 with 5,6-Br_2Bt (A, 5TS8) and TBBt (B, 1 J91). Residues located in the hinge region that often accepts halogen bonds (Glu114 and Val116), together with Lys68 and Glu81 forming salt bridge are denoted. Red arrows point halogen bonds, while magenta ones denote electrostatic interactions with Lys68/Glu81 that is most commonly observed in complexes of benzotriazole derivatives with protein kinases.

References

[1] E.E. Meyer, K.J. Rosenberg, J. Israelachvili, Recent progress in understanding hydrophobic interactions, Proc. Natl. Acad. Sci. U. S. A. 103 (2006) 15739–15746, https://doi.org/10.1073/pnas.0606422103.

[2] A. Sarkar, G.E. Kellogg, Hydrophobicity-shake flasks, protein folding and drug discovery, Curr. Top. Med. Chem. 10 (2010) 67–83, https://doi.org/10.1016/j.biotechadv.2011.08.021.Secreted.

[3] W. Kauzmann, Thermodynamics of unfolding, Nature 325 (1987) 763–764, https://doi.org/10.1038/325763a0.

[4] D. Chandler, Interfaces and the driving force of hydrophobic assembly, Nature 437 (2005) 640–647, https://doi.org/10.1038/nature04162.

[5] R.L. Baldwin, Dynamic hydration shell restores Kauzmann's 1959 explanation of how the hydrophobic factor drives protein folding, PNAS 111 (2014) 13052–13056, https://doi.org/10.1073/pnas.1414556111.

[6] R.L. Baldwin, G.D. Rose, How the hydrophobic factor drives protein folding, PNAS 113 (2016) 12462–12466, https://doi.org/10.1073/pnas.1610541113.

[7] H.S. Frank, M.W. Evans, Entropy in binary liquid mixtures; partial molal entropy in dilute solutions; structure and thermodynamics in aqueous electrolytes, J. Chem. Phys. 13 (1945) 507–532, https://doi.org/10.1063/1.1723985.

[8] M.M. Teeter, Water structure of a hydrophobic protein at atomic resolution: pentagon rings of water molecules in crystals of crambin, Proc. Natl. Acad. Sci. U. S. A. 81 (1984) 6014–6018, https://doi.org/10.1073/pnas.81.19.6014.

[9] N. Galamba, Water's structure around hydrophobic solutes and the iceberg model, J. Phys. Chem. B 117 (2013) 2153–2159, https://doi.org/10.1021/jp310649n.

[10] W. Kauzmann, Some factors in the interpretation of protein denaturation, Adv. Protein Chem. 14 (1959) 1–63, https://doi.org/10.1016/S0065-3233(08)60608-7.

[11] A. Zamyatnin, Protein volume in solution, Prog. Biophys. Mol. Biol. 24 (1972) 107–123, https://doi.org/10.1016/0079-6107(72)90005-3.

[12] A. Zamyatnin, Amino acid, peptide, and protein volume in solution, Annu. Rev. Biophys. Bioeng. 13 (1984) 145–165, https://doi.org/10.1146/annurev.bb.13.060184.001045.

[13] C. Palliser, C. A.. Parry, D, Quantitative comparison of the ability of hydropathy scales to recognize surface beta-strands in proteins., Proteins. 42 (2001) 243–255. (doi: 10.1002/1097-0134(20010201)42:2<243::AID-PROT120>3.0.CO;2-B).

[14] R.B. Hermann, Theory of hydrophobic bonding. I. the solubility of hydrocarbons in water, within the context of the significant structure theory of liquids, J. Phys. Chem. 75 (1971) 363–368, https://doi.org/10.1021/j100673a012.

[15] R.B. Hermann, Theory of hydrophobic bonding II. Correlation of hydrocarbon solubility in water with solvent cavity surface area, J. Chem. Phys. 76 (1972) 2754–2759, https://doi.org/10.1021/j100663a023.

[16] H. Reiss, Scaled particle methods in the statistical thermodynamics of fluids, Adv. Chem. Phys. (1965)https://doi.org/10.1002/9780470143551.ch1.

[17] F.H. Stillinger, Structure in aqueous solutions of nonpolar solutes from the standpoint of scaled-particle theory, J. Solut. Chem. 2 (1973) 141–158, https://doi.org/10.1007/BF00651970.

[18] O. Sinanoglu, The Solvophobic theory for the prediction of molecular conformations and biopolymer bindings in solutions with recent direct experimental tests, Int. J. Quantum Chem. XVIII (1980) 381–392, https://doi.org/10.1002/qua.560180207.

[19] K. Lum, D. Chandler, J.D. Weeks, Hydrophobicity at small and large length scales, J. Phys. Chem. B 103 (1999) 4570–4577, https://doi.org/10.1021/jp984327m.

[20] X. Chen, I. Weber, R.W. Harrison, NIH public access, J. Phys. Chem. B 112 (2008) 12073–12080, https://doi.org/10.1021/jp802795a.Hydration.

[21] J. Fidler, P.M. Rodger, Solvation structure around aqueous alcohols, J. Phys. Chem. B 103 (1999) 7695–7703, https://doi.org/10.1021/jp9907903.

[22] M. Ikeguchi, S. Shimizu, S. Nakamura, K. Shimizu, Roles of hydrogen bonding and the hard core of water on hydrophobic hydration, J. Phys. Chem. B 102 (1998) 5891–5898 (doi:10.1.1.598.3237).

[23] T. Lazaridis, Solvent reorganization energy and entropy in hydrophobic hydration, J. Phys. Chem. B 104 (2000) 4964–4979, https://doi.org/10.1021/jp994261a.

[24] N.T. Southall, K.A. Dill, A.D.J. Haymet, A view of the hydrophobic effect a view of the hydrophobic effect, J. Phys. Chem. B 106 (2002) 521–533, https://doi.org/10.1021/jp015514e.

[25] R.D.C. Barbosa, M.C. Barbosa, Hydration shell of the TS-Kappa protein: higher density than bulk water, Physica A 439 (2015) 48–58, https://doi.org/10.1016/j.physa.2015.07.026.

[26] A. Kuffel, J. Zielkiewicz, Why the solvation water around proteins is more dense than bulk water, J. Phys. Chem. B 116 (2012) 12113–12124, https://doi.org/10.1021/jp305172t.

[27] F. Merzel, J.C. Smith, High-density hydration layer of lysozymes: molecular dynamics decomposition of solution scattering data, J. Chem. Inf. Model. 45 (2005) 1593–1599, https://doi.org/10.1021/ci0502000.

[28] S.J. Perkins, X-ray and neutron scattering analyses of hydration shells: a molecular interpretation based on sequence predictions and modelling fits, Biophys. Chem. 93 (2001) 129–139, https://doi.org/10.1016/S0301-4622(01)00216-2.

[29] D.I. Svergun, S. Richards, M.H.J. Koch, Z. Sayers, S. Kuprin, G. Zaccai, Protein hydration in solution: experimental observation by x-ray and neutron scattering, Proc. Natl. Acad. Sci. U. S. A. 95 (1998) 2267–2272, https://doi.org/10.1073/pnas.95.5.2267.

[30] F. Bohm, G. Schwaab, M. Havenith, Mapping hydration water around alcohol chains by THz calorimetry, Angew. Chem. Int. Ed. 56 (2017) 9981–9985, https://doi.org/10.1002/anie.201612162.

[31] K.A. Sharp, J.M. Vanderkooi, Water in the half Shell: structure of water, focusing on angularstructure and solvation, Acc. Chem. Res. 43 (2010) 231–239, https://doi.org/10.1021/ar900154j.Water.

[32] K. Shiraga, Y. Ogawa, N. Kondo, Hydrogen bond network of water around protein investigated with terahertz and infrared spectroscopy, Biophys. J. 111 (2016) 2629–2641, https://doi.org/10.1016/j.bpj.2016.11.011.

[33] A. Esser, H. Forbert, F. Sebastiani, G. Schwaab, M. Havenith, D. Marx, Hydrophilic solvation dominates the terahertz fingerprint of amino acids in water, J. Phys. Chem. B 122 (2018) 1453–1459, https://doi.org/10.1021/acs.jpcb.7b08563.

[34] A. Leo, C. Hansch, D. Elkins, Partition coefficients and their uses, Chem. Rev. 71 (1971) 525–616, https://doi.org/10.1021/cr60274a001.

[35] A. Leo, C. Hansch, P.Y.C. Jow, Dependence of hydrophobicity of Apolar molecules on their molecular volume, J. Med. Chem. 19 (1976) 611–615, https://doi.org/10.1021/jm00227a007.

[36] T.J. Lobl, D.J. Tindall, G.R. Cunningham, P.L. Kemp, J.A. Campbell, The correlation of steroid partition coefficients with binding affinities to the rat cytoplasmic androgen receptor, rat androgen-binding protein and human testosterone estradiol-binding globulin, Ann. N. Y. Acad. Sci. 383 (1982) 477–478, https://doi.org/10.1111/j.1749-6632.1982.tb23209.x.

[37] C. Hansch, P.P. Maloney, T. Fujita, R.M. Muir, Correlation of biological activity of phenoxyacetic acids with hammett substituent constants and partition coefficient, Nature 194 (1962) 178–180, https://doi.org/10.1038/194178b0.

[38] W. Zielenkiewicz, J. Poznanski, Partial molar volumes of hydrophobic compounds—insight into the solvation Shell? Part I, J. Solut. Chem. 27 (1998) 245–254, https://doi.org/10.1023/A:1022688202224.

[39] W. Zielenkiewicz, J. Poznanski, A. Zielenkiewicz, Partial molar volumes of alkylated Uracils - insight into the solvation Shell? Part II, J. Solut. Chem. 27 (1998) 543–551, https://doi.org/10.1023/A:1022682606342.

[40] J. Poznanski, Partial molar volume as an important thermodynamic parameter. Application of uracil methyl derivatives, J. Mol. Liq. 121 (2005) 15–20, https://doi.org/10.1016/j.molliq.2004.08.021.

[41] W. Zielenkiewicz, J. Poznanski, A. Zielenkiewicz, Partial molar volumes of aqueous solutions of some halo and amino derivatives of uracil, J. Solut. Chem. 29 (2000) 757–769, https://doi.org/10.1023/A:1005169112192.

[42] W. Zielenkiewicz, J. Poznański, Partial molar volumes - insights into molecular structure, J. Mol. Liq. 81 (1999) 37–45, https://doi.org/10.1016/S0167-7322(99)00030-6.

[43] A. Andrés, M. Rosés, C. Ràfols, E. Bosch, S. Espinosa, V. Segarra, J.M. Huerta, Setup and validation of shake-flask procedures for the determination of partition coefficients (log D) from low drug amounts, Eur. J. Pharm. Sci. 76 (2015) 181–191, https://doi.org/10.1016/j.ejps.2015.05.008.

[44] P. Zień, M. Bretner, K. Zastąpiło, R. Szyszka, D. Shugar, Selectivity of 4,5,6,7-tetrabromobenzimidazole as an ATP-competitive potent inhibitor of protein kinase CK2 from various sources, Biochem. Biophys. Res. Commun. 306 (2003) 129–133, https://doi.org/10.1016/S0006-291X(03)00928-8.

[45] R. Wąsik, P. Wińska, J. Poznański, D. Shugar, Synthesis and physico-chemical properties in aqueous medium of all possible isomeric bromo analogues of benzo-1H-

triazole, potential inhibitors of protein kinases, J. Phys. Chem. B. 116 (2012) 7259–7268. doi:https://doi.org/10.1021/jp301561x.
[46] R. Wasik, M. Lebska, K. Felczak, J. Poznanski, D. Shugar, Relative role of halogen bonds and hydrophobic interactions in inhibition of human protein kinase CK2 alpha by Tetrabromobenzotriazole and some C(5)-substituted analogues, J. Phys. Chem. B 114 (2010) 10601–10611, https://doi.org/10.1021/jp102848y.
[47] P. Borowski, J. Deinert, S. Schalinski, M. Bretner, K. Ginalski, T. Kulikowski, D. Shugar, Halogenated benzimidazoles and benzotriazoles as inhibitors of the NTPase/helicase activities of hepatitis C and related viruses, Eur. J. Biochem. 270 (2003) 1645–1653, https://doi.org/10.1046/j.1432-1033.2003.03540.x.
[48] J. Poznanski, A. Najda, M. Bretner, D. Shugar, Experimental (C-13 NMR) and theoretical (ab initio molecular orbital calculations) studies on the prototropic tautomerism of benzotriazole and some derivatives symmetrically substituted on the benzene ring, J. Phys. Chem. A 111 (2007) 6501–6509, https://doi.org/10.1021/jp071611h.
[49] M. Weber, C. Hellriegel, A. Rueck, J. Wuethrich, P. Jenks, Journal of pharmaceutical and biomedical analysis organic reference materials under accreditation guidelines — describing the overall process with focus on homogeneity and stability assessment, J. Pharm. Biomed. Anal. 93 (2014) 102–110, https://doi.org/10.1016/j.jpba.2013.09.007.
[50] R. Rubio-Presa, A. Fernandez-Rodriguez, M.R. Pedrosa, F.J. Amaiz, R. Sanz, Molybdenum-catalyzed deoxygenation of Heteroaromatic N-oxides and hydroxides using Pinacol as reducing agent, Adv. Synth. Catal. 359 (2017) 1752–1757, https://doi.org/10.1002/adsc.201700071.
[51] H. Valizadeh, H. Gholipour, M. Mahmoodian, Facile synthesis of Benzotriazole derivatives using nanoparticles of Organosilane-based nitrile ionic liquid immobilized on silica and two room-temperature nitrile ionic liquids, Synth. Commun. 43 (2013) 2801–2808, https://doi.org/10.1080/00397911.2012.744840.
[52] R.H. Wiley, J. Moffat, 4,6-Dichlorobenzotriazole, J. Chem. Eng. Data 8 (1963) 279, https://doi.org/10.1021/je60017a042.
[53] K. Kopanska, A. Najda, J. Zebrowska, L. Chomicz, J. Piekarczyk, P. Myjak, M. Bretner, Synthesis and activity of 1H-benzimidazole derivatives as inhibitors of Acanthamoeba castellanii, Bioorg. Med. Chem. 12 (2004) 2617–2624, https://doi.org/10.1016/j.bmc.2004.03.022.
[54] M.W. Schmidt, K.K. Baldrige, J.A. Boatz, S.T. Elbert, M.S. Gordon, J.H. Jensen, S. Koseki, N. Matsunaga, K.A. Nguyen, S.J. Su, T.L. Windus, M. Dupuis, J.A. Montgomery, General atomic and molecular electronic-structure system, J. Comput. Chem. 14 (1993) https://doi.org/10.1002/jcc.540141112.
[55] R. Cammi, J. Tomassi, Remarks on the use of the apparent surface-charges (ACS) methods in solvation problems - iterative versus matrix-inversion procedures and the renormalization of the apparent charges, J. Comput. Chem. 16 (1995) 1449–1458, https://doi.org/10.1021/j100307a038.
[56] G.J. Tawa, I.A. Topol, S.K. Burt, R.A. Caldwell, A.A. Rashin, Calculation of the aqueous solvation free energy of the proton, J. Chem. Phys. 109 (1998) 4852–4863, https://doi.org/10.1063/1.477096.
[57] J.L. Pascualahuir, E. Silla, J. Tomasi, R. Bonaccorsi, Electrostatic interaction of a solute with a continuum - improved description of the cavity and of the surface cavity bound charge-distribution, J. Comput. Chem. 8 (1987) 778–787, https://doi.org/10.1002/jcc.540080605.
[58] A. Daina, O. Michielin, V. Zoete, SwissADME: a free web tool to evaluate pharmacokinetics, drug- likeness and medicinal chemistry friendliness of small molecules, Sci. Rep. 7 (42717) (2017) 1–13, https://doi.org/10.1038/srep42717.
[59] J.H.J. Ward, Hierarchical grouping to optimize an objective function, J. Am. Stat. Assoc. 58 (1963) 236–244, https://doi.org/10.1080/01621459.1963.10500845.
[60] R.C. Team, R: A Language and Environment for Statistical Computing, R Found. Stat. Comput, 2018.
[61] M. Winiewska, K. Kucinska, M. Makowska, J. Poznanski, D. Shugar, Thermodynamics parameters for binding of halogenated benzotriazole inhibitors of human protein kinase CK2 α, Biochim. Biophys. Acta 1854 (2015) 1708–1717, https://doi.org/10.1016/j.bbapap.2015.04.004.
[62] M.R. Eftink, The use of fluorescence methods to monitor unfolding transitions in proteins, Biophys. J. 66 (1994) 482–501, https://doi.org/10.1016/S0006-3495(94)80799-4.
[63] O. Redlich, D.M. Meyer, The molal volumes of electrolytes, Chem. Rev. 64 (1964) 221–227, https://doi.org/10.1021/cr60229a001.
[64] R. Wasik, P. Winska, J. Poznanski, D. Shugar, Isomeric mono-, Di-, and tri-Bromobenzo-1H-Triazoles as inhibitors of human protein kinase CK2 alpha, PLoS One 7 (2012)https://doi.org/10.1371/journal.pone.0048898.
[65] M. Winiewska, M. Makowska, P. Maj, M. Wielechowska, M. Bretner, J. Poznanski, D. Shugar, Thermodynamic parameters for binding of some halogenated inhibitors of human protein kinase CK2, Biochem. Biophys. Res. Commun. 456 (2015) 282–287, https://doi.org/10.1016/j.bbrc.2014.11.072.
[66] M. Winiewska, E. Bugajska, J. Poznanski, ITC-derived binding affinity may be biased due to titrant (nano)-aggregation. Binding of halogenated benzotriazoles to the catalytic domain of human protein kinase CK2, PLoS One 12 (2017)https://doi.org/10.1371/journal.pone.0173260.
[67] P. Auffinger, A. Hays, E. Westhof, P.S. Ho, Halogen bonds in biological molecules, Proc. Natl. Acad. Sci. U. S. A. 101 (2004) 16789–16794, https://doi.org/10.1073/pnas.0407607101.
[68] J. Poznanski, D. Shugar, Halogen bonding at the ATP binding site of protein kinases: Preffered geometry and topology of ligand binding, Biochim. Biophys. Acta - Proteins Proteomics. 1834 (2013) 1381–1386, https://doi.org/10.1016/j.bbapap.2013.01.026.
[69] J. Poznanski, M. Winiewska, H. Czapinska, A. Poznanska, D. Shugar, Halogen bonds involved in binding of halogenated ligands by protein kinases, Acta Biochim. Pol. 63 (2016) 203–214, https://doi.org/10.18388/abp.2015_1106.
[70] P. Zhou, F. Tian, J. Zou, Z. Shang, Rediscovery of halogen bonds in protein-ligand complexes, Mini-Reviews Med. Chem. 10 (2010) 309–314, https://doi.org/10.2174/138955710791331016.
[71] A. Daina, O. Michielin, V. Zoete, iLOGP: a simple, robust, and efficient description of n-octanol/water partition coefficient for drug design using the GB/SA approach, J. Chem. Inf. Model. 54 (2014) 3284–3301, https://doi.org/10.1021/ci500467k.
[72] G.W. Snedecor, W.G. Cochran, Statistical Methods Applied to Experiments in Agriculture and Biology, 1989.
[73] K. Valko, C. Bevan, D. Reynolds, Chromatographic hydrophobicity index by fast-gradient RP-HPLC: a high-throughput alternative to log P/log D, Anal. Chem. 69 (1997) 2022–2029, https://doi.org/10.1021/ac961242d.
[74] F. Lombardo, M.Y. Shalaeva, K.A. Tupper, F. Gao, ElogDoct: a tool for lipophilicity determination in drug discovery. 2. Basic and neutral compounds, J. Med. Chem. 44 (2001) 2490–2497, https://doi.org/10.1021/jm0100990.
[75] K. Valko, Application of high-performance liquid chromatography based measurements of lipophilicity to model biological distribution, J. Chromatogr. A 1037 (2004) 299–310, https://doi.org/10.1016/j.chroma.2003.10.084.
[76] R. Battistutta, M. Mazzorana, S. Samo, Z. Kazimierczuk, G. Zanotti, L.A. Pinna, Inspecting the structure-activity relationship of protein kinase CK2 inhibitors derived from tetrabromo-benzimidazole, Chem. Biol. 12 (2005) 1211–1219, https://doi.org/10.1016/j.chembiol.2005.08.015.
[77] R. Battistutta, Structural bases of protein kinase CK2 inhibition, Cell. Mol. Life Sci. 66 (2009) 1868–1889, https://doi.org/10.1007/s00018-009-9155-x.
[78] E.D. Moliner, N.R. Brown, L.N. Johnson, Alternative binding modes of an inhibitor to two different kinases, Eur. J. Biochem. 270 (2003) 3174–3181, https://doi.org/10.1046/j.1432-1033.2003.03697.x.
[79] R. Battistutta, E.D. Moliner, S. Samo, G. Zanotti, L.A. Pinna, Structural features underlying selective inhibition of protein kinase CK2 by ATP site-directed tetrabromo-2-benzotriazole, Protein Sci. 10 (2001) 2200–2206, https://doi.org/10.1110/ps.19601.